

Precision measurement of the integrated luminosity of the data taken by BESIII at center of mass energies between 3.810 GeV and 4.600 GeV

M. Ablikim¹, M. N. Achasov^{9,a}, X. C. Ai¹, O. Albayrak⁵, M. Albrecht⁴, D. J. Ambrose⁴⁴, A. Amoroso^{48A,48C}, F. F. An¹, Q. An⁴⁵, J. Z. Bai¹, R. Baldini Ferroli^{20A}, Y. Ban³¹, D. W. Bennett¹⁹, J. V. Bennett⁵, M. Bertani^{20A}, D. Bettoni^{21A}, J. M. Bian⁴³, F. Bianchi^{48A,48C}, E. Boger^{23,h}, O. Bondarenko²⁵, I. Boyko²³, R. A. Briere⁵, H. Cai⁵⁰, X. Cai¹, O. Cakir^{40A,b}, A. Calcaterra^{20A}, G. F. Cao¹, S. A. Cetin^{40B}, J. F. Chang¹, G. Chelkov^{23,c}, G. Chen¹, H. S. Chen¹, H. Y. Chen², J. C. Chen¹, M. L. Chen¹, S. J. Chen²⁹, X. Chen¹, X. R. Chen²⁶, Y. B. Chen¹, H. P. Cheng¹⁷, X. K. Chu³¹, G. Cibinetto^{21A}, D. Cronin-Hennessy⁴³, H. L. Dai¹, J. P. Dai³⁴, A. Dbeyssi¹⁴, D. Dedovich²³, Z. Y. Deng¹, A. Denig²², I. Denysenko²³, M. Destefanis^{48A,48C}, F. De Mori^{48A,48C}, Y. Ding²⁷, C. Dong³⁰, J. Dong¹, L. Y. Dong¹, M. Y. Dong¹, S. X. Du⁵², P. F. Duan¹, J. Z. Fan³⁹, J. Fang¹, S. S. Fang¹, X. Fang⁴⁵, Y. Fang¹, L. Fava^{48B,48C}, F. Feldbauer²², G. Felici^{20A}, C. Q. Feng⁴⁵, E. Fioravanti^{21A}, M. Fritsch^{14,22}, C. D. Fu¹, Q. Gao¹, Y. Gao³⁹, Z. Gao⁴⁵, I. Garzia^{21A}, C. Geng⁴⁵, K. Goetzen¹⁰, W. X. Gong¹, W. Gradl²², M. Greco^{48A,48C}, M. H. Gu¹, Y. T. Gu¹², Y. H. Guan¹, A. Q. Guo¹, L. B. Guo²⁸, Y. Guo¹, Y. P. Guo²², Z. Haddadi²⁵, A. Hafner²², S. Han⁵⁰, Y. L. Han¹, X. Q. Hao¹⁵, F. A. Harris⁴², K. L. He¹, Z. Y. He³⁰, T. Held⁴, Y. K. Heng¹, Z. L. Hou¹, C. Hu²⁸, H. M. Hu¹, J. F. Hu^{48A,48C}, T. Hu¹, Y. Hu¹, G. M. Huang⁶, G. S. Huang⁴⁵, H. P. Huang⁵⁰, J. S. Huang¹⁵, X. T. Huang³³, Y. Huang²⁹, T. Hussain⁴⁷, Q. Ji¹, Q. P. Ji³⁰, X. B. Ji¹, X. L. Ji¹, L. L. Jiang¹, L. W. Jiang⁵⁰, X. S. Jiang¹, J. B. Jiao³³, Z. Jiao¹⁷, D. P. Jin¹, S. Jin¹, T. Johansson⁴⁹, A. Julin⁴³, N. Kalantar-Nayestanaki²⁵, X. L. Kang¹, X. S. Kang³⁰, M. Kavatsyuk²⁵, B. C. Ke⁵, R. Kliemt¹⁴, B. Kloss²², O. B. Kolcu^{40B,d}, B. Kopf⁴, M. Kornicer⁴², W. Kuehn²⁴, A. Kupsc⁴⁹, W. Lai¹, J. S. Lange²⁴, M. Lara¹⁹, P. Larin¹⁴, C. Leng^{48C}, C. H. Li¹, Cheng Li⁴⁵, D. M. Li⁵², F. Li¹, G. Li¹, H. B. Li¹, J. C. Li¹, Jin Li³², K. Li¹³, K. Li³³, Lei Li³, P. R. Li⁴¹, T. Li³³, W. D. Li¹, W. G. Li¹, X. L. Li³³, X. M. Li¹², X. N. Li¹, X. Q. Li³⁰, Z. B. Li³⁸, H. Liang⁴⁵, Y. F. Liang³⁶, Y. T. Liang²⁴, G. R. Liao¹¹, D. X. Lin¹⁴, B. J. Liu¹, C. X. Liu¹, F. H. Liu³⁵, Fang Liu¹, Feng Liu⁶, H. B. Liu¹², H. H. Liu¹⁶, H. H. Liu¹, H. M. Liu¹, J. Liu¹, J. P. Liu⁵⁰, J. Y. Liu¹, K. Liu³⁹, K. Y. Liu²⁷, L. D. Liu³¹, P. L. Liu¹, Q. Liu⁴¹, S. B. Liu⁴⁵, X. Liu²⁶, X. X. Liu⁴¹, Y. B. Liu³⁰, Z. A. Liu¹, Zhiqiang Liu¹, Zhiqing Liu²², H. Loehner²⁵, X. C. Lou^{1,e}, H. J. Lu¹⁷, J. G. Lu¹, R. Q. Lu¹⁸, Y. Lu¹, Y. P. Lu¹, C. L. Luo²⁸, M. X. Luo⁵¹, T. Luo²⁸, X. L. Luo¹, M. Lv¹, X. R. Lyu⁴¹, F. C. Ma²⁷, H. L. Ma¹, L. L. Ma³³, Q. M. Ma¹, S. Ma¹, T. Ma¹, X. N. Ma³⁰, X. Y. Ma¹, F. E. Maas¹⁴, M. Maggiora^{48A,48C}, Q. A. Malik⁴⁷, Y. J. Mao³¹, Z. P. Mao¹, S. Marcello^{48A,48C}, J. G. Messendorp²⁵, J. Min¹, T. J. Min¹, R. E. Mitchell¹⁹, X. H. Mo¹, Y. J. Mo⁶, C. Morales Morales¹⁴, K. Moriya¹⁹, N. Yu. Muchnoi^{9,a}, H. Muramatsu⁴³, Y. Nefedov²³, F. Nerling¹⁴, I. B. Nikolaev^{9,a}, Z. Ning¹, S. Nisar⁸, S. L. Niu¹, X. Y. Niu¹, S. L. Olsen³², Q. Ouyang¹, S. Pacetti^{20B}, P. Patteri^{20A}, M. Pelizaeus⁴, H. P. Peng⁴⁵, K. Peters¹⁰, J. L. Ping²⁸, R. G. Ping¹, R. Poling⁴³, Y. N. Pu¹⁸, M. Qi²⁹, S. Qian¹, C. F. Qiao⁴¹, L. Q. Qin³³, N. Qin⁵⁰, X. S. Qin¹, Y. Qin³¹, Z. H. Qin¹, J. F. Qiu¹, K. H. Rashid⁴⁷, C. F. Redmer²², H. L. Ren¹⁸, M. Ripka²², G. Rong¹, X. D. Ruan¹², V. Santoro^{21A}, A. Sarantsev^{23,f}, M. Savrie^{21B}, K. Schoenning⁴⁹, S. Schumann²², W. Shan³¹, M. Shao⁴⁵, C. P. Shen²², P. X. Shen³⁰, X. Y. Shen¹, H. Y. Sheng¹, W. M. Song¹, X. Y. Song¹, S. Sosio^{48A,48C}, S. Spataro^{48A,48C}, G. X. Sun¹, J. F. Sun¹⁵, S. S. Sun¹, Y. J. Sun⁴⁵, Y. Z. Sun¹, Z. J. Sun¹, Z. T. Sun¹⁹, C. J. Tang³⁶, X. Tang¹, I. Tapan^{40C}, E. H. Thorndike⁴⁴, M. Tiemens²⁵, D. Toth⁴³, M. Ullrich²⁴, I. Uman^{40B}, G. S. Varner⁴², B. Wang³⁰, B. L. Wang⁴¹, D. Wang³¹, D. Y. Wang³¹, K. Wang¹, L. L. Wang¹, L. S. Wang¹, M. Wang³³, P. Wang¹, P. L. Wang¹, Q. J. Wang¹, S. G. Wang³¹, W. Wang¹, X. F. Wang³⁹, Y. D. Wang^{20A}, Y. F. Wang¹, Y. Q. Wang²², Z. Wang¹, Z. G. Wang¹, Z. H. Wang⁴⁵, Z. Y. Wang¹, T. Weber²², D. H. Wei¹¹, J. B. Wei³¹, P. Weidenkaff²², S. P. Wen¹, U. Wiedner⁴, M. Wolke⁴⁹, L. H. Wu¹, Z. Wu¹, L. G. Xia³⁹, Y. Xia¹⁸, D. Xiao¹, Z. J. Xiao²⁸, Y. G. Xie¹, Q. L. Xiu¹, G. F. Xu¹, L. Xu¹, Q. J. Xu¹³, Q. N. Xu⁴¹, X. P. Xu³⁷, L. Yan⁴⁵, W. B. Yan⁴⁵, W. C. Yan⁴⁵, Y. H. Yan¹⁸, H. X. Yang¹, L. Yang⁵⁰, Y. Yang⁶, Y. X. Yang¹¹, H. Ye¹, M. Ye¹, M. H. Ye⁷, J. H. Yin¹, B. X. Yu¹, C. X. Yu³⁰, H. W. Yu³¹, J. S. Yu²⁶, C. Z. Yuan¹, W. L. Yuan²⁹, Y. Yuan¹, A. Yuncu^{40B,g}, A. A. Zafar⁴⁷, A. Zallo^{20A}, Y. Zeng¹⁸, B. X. Zhang¹, B. Y. Zhang¹, C. Zhang²⁹, C. C. Zhang¹, D. H. Zhang¹, H. H. Zhang³⁸, H. Y. Zhang¹, J. J. Zhang¹, J. L. Zhang¹, J. Q. Zhang¹, J. W. Zhang¹, J. Y. Zhang¹, J. Z. Zhang¹, K. Zhang¹, L. Zhang¹, S. H. Zhang¹, X. Y. Zhang³³, Y. Zhang¹, Y. H. Zhang¹, Y. T. Zhang⁴⁵, Z. H. Zhang⁶, Z. P. Zhang⁴⁵, Z. Y. Zhang⁵⁰, G. Zhao¹, J. W. Zhao¹, J. Y. Zhao¹, J. Z. Zhao¹, Lei Zhao⁴⁵, Ling Zhao¹, M. G. Zhao³⁰, Q. Zhao¹, Q. W. Zhao¹, S. J. Zhao⁵², T. C. Zhao¹, Y. B. Zhao¹, Z. G. Zhao⁴⁵, A. Zhemchugov^{23,h}, B. Zheng⁴⁶, J. P. Zheng¹, W. J. Zheng³³, Y. H. Zheng⁴¹, B. Zhong²⁸, L. Zhou¹, Li Zhou³⁰, X. Zhou⁵⁰, X. K. Zhou⁴⁵, X. R. Zhou⁴⁵, X. Y. Zhou¹, K. Zhu¹, K. J. Zhu¹, S. Zhu¹, X. L. Zhu³⁹, Y. C. Zhu⁴⁵, Y. S. Zhu¹, Z. A. Zhu¹, J. Zhuang¹, L. Zotti^{48A,48C}, B. S. Zou¹, J. H. Zou¹

(BESIII Collaboration)

¹ Institute of High Energy Physics, Beijing 100049, People's Republic of China

² Beihang University, Beijing 100191, People's Republic of China

³ Beijing Institute of Petrochemical Technology, Beijing 102617, People's Republic of China

⁴ Bochum Ruhr-University, D-44780 Bochum, Germany

⁵ Carnegie Mellon University, Pittsburgh, Pennsylvania 15213, USA

⁶ Central China Normal University, Wuhan 430079, People's Republic of China

⁷ China Center of Advanced Science and Technology, Beijing 100190, People's Republic of China

⁸ COMSATS Institute of Information Technology, Lahore, Defence Road, Off Raiwind Road, 54000 Lahore, Pakistan

⁹ G.I. Budker Institute of Nuclear Physics SB RAS (BINP), Novosibirsk 630090, Russia

¹⁰ GSI Helmholtzcentre for Heavy Ion Research GmbH, D-64291 Darmstadt, Germany

¹¹ Guangxi Normal University, Guilin 541004, People's Republic of China

¹² GuangXi University, Nanning 530004, People's Republic of China

¹³ Hangzhou Normal University, Hangzhou 310036, People's Republic of China

¹⁴ Helmholtz Institute Mainz, Johann-Joachim-Becher-Weg 45, D-55099 Mainz, Germany

¹⁵ Henan Normal University, Xinxiang 453007, People's Republic of China

¹⁶ Henan University of Science and Technology, Luoyang 471003, People's Republic of China

¹⁷ Huangshan College, Huangshan 245000, People's Republic of China

¹⁸ Hunan University, Changsha 410082, People's Republic of China

- ¹⁹ *Indiana University, Bloomington, Indiana 47405, USA*
- ²⁰ (A) *INFN Laboratori Nazionali di Frascati, I-00044, Frascati, Italy; (B) INFN and University of Perugia, I-06100, Perugia, Italy*
- ²¹ (A) *INFN Sezione di Ferrara, I-44122, Ferrara, Italy; (B) University of Ferrara, I-44122, Ferrara, Italy*
- ²² *Johannes Gutenberg University of Mainz, Johann-Joachim-Becher-Weg 45, D-55099 Mainz, Germany*
- ²³ *Joint Institute for Nuclear Research, 141980 Dubna, Moscow region, Russia*
- ²⁴ *Justus Liebig University Giessen, II. Physikalisches Institut, Heinrich-Buff-Ring 16, D-35392 Giessen, Germany*
- ²⁵ *KVI-CART, University of Groningen, NL-9747 AA Groningen, The Netherlands*
- ²⁶ *Lanzhou University, Lanzhou 730000, People's Republic of China*
- ²⁷ *Liaoning University, Shenyang 110036, People's Republic of China*
- ²⁸ *Nanjing Normal University, Nanjing 210023, People's Republic of China*
- ²⁹ *Nanjing University, Nanjing 210093, People's Republic of China*
- ³⁰ *Nankai University, Tianjin 300071, People's Republic of China*
- ³¹ *Peking University, Beijing 100871, People's Republic of China*
- ³² *Seoul National University, Seoul, 151-747 Korea*
- ³³ *Shandong University, Jinan 250100, People's Republic of China*
- ³⁴ *Shanghai Jiao Tong University, Shanghai 200240, People's Republic of China*
- ³⁵ *Shanxi University, Taiyuan 030006, People's Republic of China*
- ³⁶ *Sichuan University, Chengdu 610064, People's Republic of China*
- ³⁷ *Soochow University, Suzhou 215006, People's Republic of China*
- ³⁸ *Sun Yat-Sen University, Guangzhou 510275, People's Republic of China*
- ³⁹ *Tsinghua University, Beijing 100084, People's Republic of China*
- ⁴⁰ (A) *Istanbul Aydin University, 34295 Sefakoy, Istanbul, Turkey; (B) Dogus University, 34722 Istanbul, Turkey; (C) Uludag University, 16059 Bursa, Turkey*
- ⁴¹ *University of Chinese Academy of Sciences, Beijing 100049, People's Republic of China*
- ⁴² *University of Hawaii, Honolulu, Hawaii 96822, USA*
- ⁴³ *University of Minnesota, Minneapolis, Minnesota 55455, USA*
- ⁴⁴ *University of Rochester, Rochester, New York 14627, USA*
- ⁴⁵ *University of Science and Technology of China, Hefei 230026, People's Republic of China*
- ⁴⁶ *University of South China, Hengyang 421001, People's Republic of China*
- ⁴⁷ *University of the Punjab, Lahore-54590, Pakistan*
- ⁴⁸ (A) *University of Turin, I-10125, Turin, Italy; (B) University of Eastern Piedmont, I-15121, Alessandria, Italy; (C) INFN, I-10125, Turin, Italy*
- ⁴⁹ *Uppsala University, Box 516, SE-75120 Uppsala, Sweden*
- ⁵⁰ *Wuhan University, Wuhan 430072, People's Republic of China*
- ⁵¹ *Zhejiang University, Hangzhou 310027, People's Republic of China*
- ⁵² *Zhengzhou University, Zhengzhou 450001, People's Republic of China*
- ^a *Also at the Novosibirsk State University, Novosibirsk, 630090, Russia*
- ^b *Also at Ankara University, 06100 Tandogan, Ankara, Turkey*
- ^c *Also at the Moscow Institute of Physics and Technology, Moscow 141700, Russia and at the Functional Electronics Laboratory, Tomsk State University, Tomsk, 634050, Russia*
- ^d *Currently at Istanbul Arel University, 34295 Istanbul, Turkey*
- ^e *Also at University of Texas at Dallas, Richardson, Texas 75083, USA*
- ^f *Also at the NRC "Kurchatov Institute", PNPI, 188300, Gatchina, Russia*
- ^g *Also at Bogazici University, 34342 Istanbul, Turkey*
- ^h *Also at the Moscow Institute of Physics and Technology, Moscow 141700, Russia*

From December 2011 to May 2014, about 5 fb^{-1} of data were taken with the BESIII detector at center-of-mass energies between 3.810 GeV and 4.600 GeV to study the charmoniumlike states and higher excited charmonium states. The time-integrated luminosity of the collected data sample is measured to a precision of 1% by analyzing events produced by the large-angle Bhabha scattering process.

PACS numbers: 13.66.Jn

I. INTRODUCTION

As a τ -charm factory, the BESIII experiment has collected the world's largest sample of e^+e^- collision data at center-of-mass (CM) energies between 3.810 GeV and 4.600 GeV. In

this energy region, the charmoniumlike states and higher excited charmonium states are produced copiously, which makes comprehensive studies possible.

The charmoniumlike states discovered in recent years have drawn great attention of both theorists and experimentalists

for their exotic properties, as reviewed *e.g.* in Ref. [1]. Being well above the open charm threshold, the strong coupling of these states to hidden charm processes makes their interpretation as conventional charmonium states very difficult. On the other hand, the theory of the strong interaction, Quantum Chromodynamics (QCD), does not prohibit the existence of exotic states beyond the quark model, *e.g.* molecular states, tetraquark states, hybrid states, *etc.* Either the verification or the exclusion of the existence of such states will help to evaluate the quark model and better understand QCD. Even though some states have been identified as higher excited charmonium states, such as the $\psi(4040)$, $\psi(4160)$, and $\psi(4415)$, their large widths and the interference with each other make their precise study complicated. In addition, the relationship between the charmoniumlike states and higher excited charmonium states is still not clear. The precise knowledge of the time-integrated luminosity is essential for quantitative analysis of these states.

In this paper, we present a measurement of the integrated luminosity based on the analysis of the Bhabha scattering process $e^+e^- \rightarrow (\gamma)e^+e^-$. A similar method has been used in the luminosity measurement of $\psi(3770)$ data at BESIII [2]. The process has a simple and clean signature and a large production cross section, which allows for a small systematic and a negligible statistical uncertainty. A cross check of the result is performed by analyzing the di-gamma process $e^+e^- \rightarrow \gamma\gamma$.

II. THE DETECTOR

BESIII is a general purpose detector which covers 93% of the solid angle and operates at the e^+e^- collider BEPCII. A detailed description of the facilities is given in Ref. [3]. The detector consists of four main components: (a) A small-cell, helium-based main drift chamber (MDC) with 43 layers provides an average single-hit resolution of 135 μm , and a momentum resolution of 0.5% for charged tracks at 1 GeV/ c in a 1 T magnetic field. (b) An electro-magnetic calorimeter (EMC), consisting of 6240 CsI(Tl) crystals in a cylindrical structure (barrel and two endcaps). The energy resolution for 1.0 GeV photons is 2.5% (5%) in the barrel (endcaps), while the position resolution is 6 mm (9 mm) in the barrel (endcaps). (c) A time-of-flight system (TOF), constructed of 5 cm thick plastic scintillators, arranged in 88 detectors of 2.4 m length in two layers in the barrel and 96 fan-shaped detectors in the endcaps. The barrel (endcap) time resolution of 80 ps (110 ps) provides $2\sigma K/\pi$ separation for momenta up to about 1.0 GeV/ c . (d) A muon counter (MUC), consisting of nine layers of resistive plate chambers in the barrel and eight layers for each endcap. It is incorporated in the iron return yoke of the superconducting magnet. Its position resolution is about 2 cm. A GEANT4 [4, 5] based detector simulation package has been developed to model the detector response. Due to the crossing angle of the beams at the interaction point, the e^+e^- CM system is slightly boosted with respect to the laboratory frame.

III. DATA SAMPLE AND MONTE CARLO SIMULATION

Twenty-one data samples have been taken at CM energies between 3.810 GeV and 4.600 GeV. Six of the data sets exceed the others in accumulated statistics by an order of magnitude. These samples were taken on the peaks of charmoniumlike states, like the Y(4260), Y(4360), and Y(4630), or higher excited charmonium states, like $\psi(4040)$, and $\psi(4415)$, in order to study these resonances and their decays in great detail. The data samples taken at the other CM energies serve as scan points to study the behavior of the cross section around these resonances. All individual data samples are listed in Table I.

At each energy point, one million Bhabha events were generated using the BABAYAGA3.5 [6] generator with the options presented in Table II. For the BABAYAGA3.5 generator, the uncertainty in calculating the cross section is 0.5%, which meets the demand of the total uncertainty of luminosity measurement. The kinematic distributions of the final state particles from the BABAYAGA3.5 generator are consistent with those from data. In the simulation, the scattering angles of the final state particles were limited to a range from 20 degrees to 160 degrees, which slightly exceeds the sensitive volume of the detector, in order to save on computing resources. An energy threshold of 0.04 GeV was applied on the final state particles. The acolinearity of the events has not been constrained. Finally, the generation was taking into account the running of the electromagnetic coupling constant and final state radiation (FSR).

To study the background and optimize the event selection criteria, an inclusive Monte Carlo (MC) sample corresponding to a luminosity of 500 pb^{-1} at the CM energy of 4.260 GeV was generated, in which the QED processes, the continuum production of hadrons, and the initial state radiation (ISR) to J/ψ and $\psi(3686)$ resonance process were included. The BABAYAGA3.5 generator was used to simulate the QED processes, signal and background. Other processes, such as the decays of the J/ψ , were generated with specialized models that have been packaged and customized for the BESIII Offline Software System (BOSS) (see [7] for an overview).

IV. EVENT SELECTION AND RESULT

Signal candidates are required to have exactly two oppositely charged tracks. The tracks must originate from a cylindrical volume, centered around the interaction point, which is defined by a radius of 1 cm perpendicular to the beam axis and a length of ± 10 cm along the beam axis. In addition, the charged tracks are required to be within $|\cos\theta| < 0.8$, where θ is the polar angle, measured by the MDC. Without applying further particle identification, the tracks are assigned as electron and positron depending on their charge. The deposited energies of electron and positron in EMC must be larger than $\frac{\sqrt{s}}{4.26} \times 1.55$ (GeV) to remove the di-muon background, where \sqrt{s} is the CM energy in GeV; the momenta of electron and positron are required to be larger than $\frac{\sqrt{s}}{4.26} \times 2$ (GeV/ c), to

TABLE I. Center-of-mass energy, luminosity obtained from the nominal measurement (L), cross check results (L_{ck}), and relative differences between the two results. The uncertainties are statistical only. Superscripts indicate separate samples acquired at the same CM energy.

CM energy (GeV)	L (pb $^{-1}$)	L_{ck} (pb $^{-1}$)	Relative difference (%)
3.810	50.54±0.03	50.11±0.08	-0.85±0.17
3.900	52.61±0.03	52.57±0.08	-0.08±0.17
4.009	481.96±0.01	480.54±0.23	-0.30±0.05
4.090	52.63±0.03	52.37±0.08	-0.49±0.17
4.190	43.09±0.03	43.08±0.08	-0.03±0.20
4.210	54.55±0.03	54.27±0.09	-0.62±0.18
4.220	54.13±0.03	54.22±0.09	+0.17±0.18
4.230 ¹	44.40±0.03	44.64±0.08	+0.54±0.20
4.230 ²	1047.34±0.14	1041.56±0.37	-0.56±0.04
4.245	55.59±0.04	55.52±0.09	-0.13±0.18
4.260 ¹	523.74±0.10	524.57±0.26	+0.16±0.06
4.260 ²	301.93±0.08	301.11±0.20	-0.28±0.08
4.310	44.90±0.03	45.29±0.08	+0.87±0.19
4.360	539.84±0.10	541.38±0.28	+0.29±0.06
4.390	55.18±0.04	55.27±0.09	+0.16±0.18
4.420 ¹	44.67±0.03	44.77±0.08	+0.22±0.20
4.420 ²	1028.89±0.13	1029.63±0.37	+0.07±0.04
4.470	109.94±0.04	109.51±0.13	-0.39±0.13
4.530	109.98±0.04	109.47±0.13	-0.46±0.13
4.575	47.67±0.03	47.57±0.08	-0.21±0.18
4.600	566.93±0.11	563.45±0.28	-0.62±0.06

TABLE II. Options for the BABAYAGA3.5 generator used to generate the simulated MC data samples.

Parameters	Value
Ebeam	2.130 GeV or others
MinThetaAngle	20°
MaxThetaAngle	160°
MinimumEnergy	0.04 GeV
MaximumAcollinearity	180°
RunningAlpha	1
FSR switch	1

suppress background events from lighter vector resonances produced in the ISR process, such as J/ψ , $\psi(3686)$ and other resonances, decaying into e^+e^- pairs. For the data sample with a CM energy of 3.810 or 3.910 GeV, the effect of the remaining $\psi(3686)$ events is studied by applying a 20% larger momentum requirement, and is found to be negligible. The requirements on the deposited energies and momenta are not optimized in detail, as the number of the signal events in such an analysis is large enough. All the variables mentioned above are determined in the initial e^+e^- CM frame. The ratio of the number of remaining background events to the number of signal events, estimated from the inclusive MC sample, is found to be less than 2×10^{-4} , which is negligible. Thus all the selected events are taken as Bhabha events.

Figure 1 shows the comparisons between data and MC simulation for the kinematic variables of the leptons by taking data at the CM energy of 4.260 GeV as an example. Reasonable agreement is observed in the angular and momentum

distributions. The striking difference between data and simulation found in the distributions of energies deposited by the leptons in the EMC emerges from imperfections in the simulation of the energy response of individual detector channels. At the CM energies analyzed in this work, a single shower in the calorimeter can be so energetic that the deposited energy per crystal exceeds the dynamic range of the analog-to-digital converter (ADC), causing individual ADC channels to saturate. In the analysis presented in this report, conditions applied on the energy deposits are not affected. Relevant deviations between data and MC are considered as contributions to the systematic uncertainties.

The integrated luminosity is calculated with

$$L = \frac{N_{\text{Bhabha}}^{\text{obs}}}{\sigma_{\text{Bhabha}} \times \epsilon}, \quad (1)$$

where $N_{\text{Bhabha}}^{\text{obs}}$ is the number of observed Bhabha events, σ_{Bhabha} is the cross section of the Bhabha process, and ϵ is the efficiency determined by analyzing the signal MC sample. The cross sections are calculated with the BABAYAGA3.5 generator using the parameters listed in Table II and decrease with increasing energies. The efficiencies are almost independent of the CM energy, as intended by the choice of relative conditions on lepton momenta and deposited energies. The luminosity results calculated with Equation 1 are listed in Table I. The statistical accuracy of the resulting integrated luminosity is better than 0.1% at all energy points.

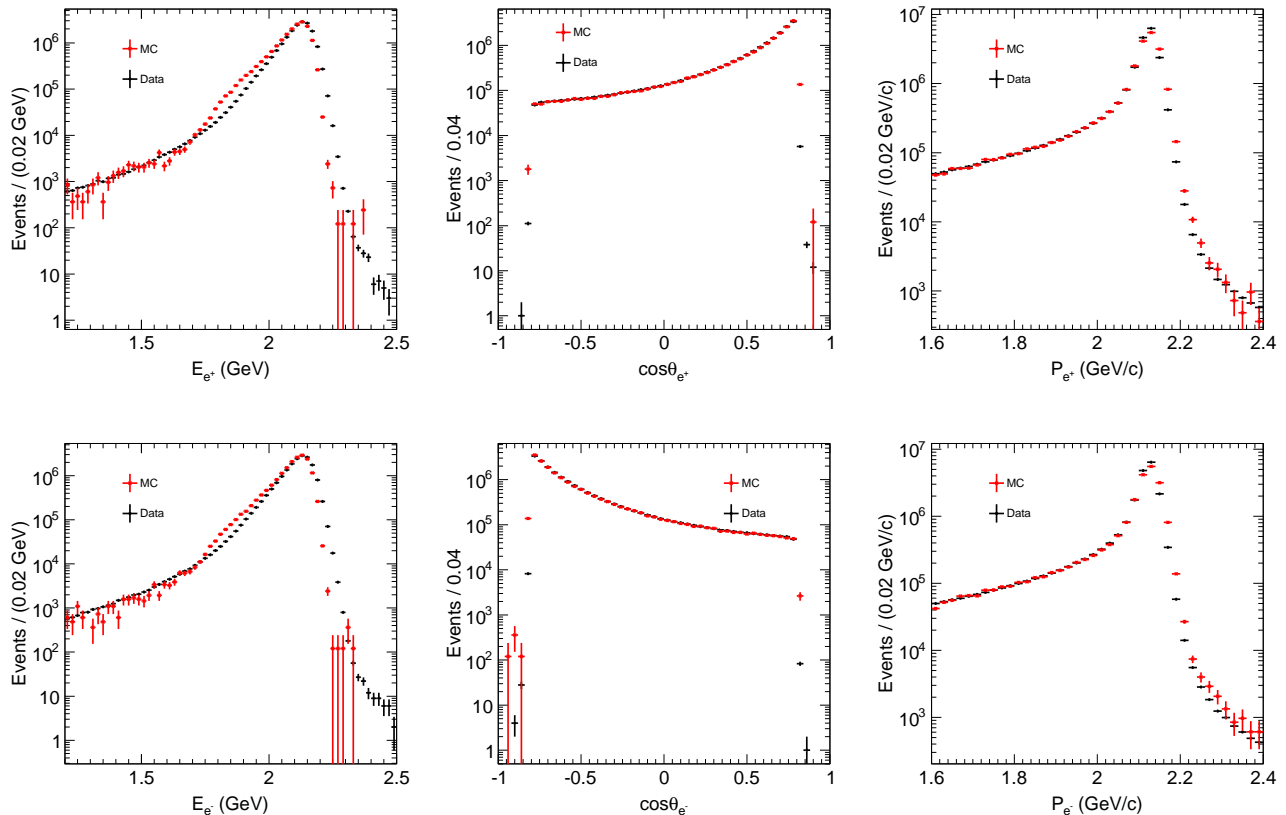


FIG. 1. Comparison between data and MC simulation at the CM energy of 4.260 GeV. The top row is for positron and the bottom row for electron. From left to right, the plots show the distribution of deposited energy in EMC, the distribution of the cosine of the polar angle measured by the MDC, and the distribution of the track momentum from the MDC. Black dots with error bars illustrate data and the red ones are MC simulation. Note that the y-axis is in logarithmic scale and the MC is normalized to data by the number of events for each sub-plot. When drawing the distribution of one variable, the requirements on the other variables are applied.

V. SYSTEMATIC UNCERTAINTY

The following sources of systematic uncertainties are considered: the uncertainty of the tracking efficiency, the uncertainty related to the requirements on the kinematic variables, the statistical uncertainty of the MC sample, the uncertainty of the beam energy measurement, the uncertainty of the trigger efficiency, and the systematic uncertainty of the event generator.

To estimate the systematic uncertainty related to the tracking efficiency, the Bhabha event sample is selected using information from the EMC only, without using the tracking information in the MDC. The selection criteria are: at least two clusters in the EMC for each candidate, and the two most energetic clusters are assumed to originate from the e^+e^- pair; the deposited energies of the two clusters are required to be larger than $\frac{\sqrt{s}}{4.26} \times 1.8$ (GeV). At CM energies above 4.420 GeV, the requirement is changed to $\frac{\sqrt{s}}{4.26} \times 1.55$ (GeV). This adjustment allows to avoid additional systematic uncertainties which would be introduced by the deviation of data and simulation in the deposited energy in the EMC, as discussed in

Sec.IV. The polar angle of each cluster is required to be within $|\cos\theta^{\text{EMC}}| < 0.8$, where θ^{EMC} is the polar angle measured by the EMC; to remove the background from the di-photon process, $\Delta\phi$ is required to be in the range of $[-40^\circ, -5^\circ]$ or $[5^\circ, 40^\circ]$, where $\Delta\phi = |\phi_1 - \phi_2| - 180^\circ$ and $\phi_{1,2}$ are the azimuthal angles of the clusters in the EMC boosted to the CM frame. The efficiency that the selected Bhabha events pass through the track requirements applied in the nominal analysis is calculated for both data and MC sample, and the difference between them is taken as the systematic uncertainty connected to the tracking efficiency.

The systematic uncertainty in the requirement on the polar angle is estimated by changing the requirement from $|\cos\theta| < 0.8$ to $|\cos\theta| < 0.7$. The difference between the resulting luminosity and nominal one is taken as the associated systematic uncertainty. The systematic uncertainty caused by the requirement on the energy deposited in the EMC is estimated by changing the requirement from $\frac{\sqrt{s}}{4.26} \times 1.55$ (GeV) to $\frac{\sqrt{s}}{4.26} \times 1.71$ (GeV). The systematic uncertainty caused by the requirement on the momentum is estimated by changing the requirement from $\frac{\sqrt{s}}{4.26} \times 2$ (GeV/c) to $\frac{\sqrt{s}}{4.26} \times 2.06$ (GeV/c).

The ranges are picked as these cause the largest deviations from the nominal luminosity result near the requirements applied.

The statistical uncertainty of the efficiency determined from MC simulations is 0.25%. The CM energy is determined using $e^+e^- \rightarrow (\gamma)\mu^+\mu^-$ events. The invariant mass of the di-muon system is calculated taking into account ISR and FSR effects [8]. The difference between the CM energy listed in Table I and the one measured with di-muon process is about 2 MeV, and the corresponding systematic uncertainty is estimated by changing the CM energy by 2 MeV in the MC simulation. The trigger efficiency for the Bhabha process is 100% with an uncertainty of less than 0.1% [9]. The theoretical uncertainty of the cross section calculated by the BABAYAGA3.5 generator is given as 0.5% [6].

The same systematic uncertainty estimation method is applied to all the sub-samples. The largest relative uncertainty among them is taken as the associated uncertainty for all the sub-samples. The systematic uncertainties considered in this work are summarized in Table III. By assuming the sources of the systematic uncertainties to be uncorrelated, the total uncertainty is calculated as 0.97% by adding the contributions in quadrature.

TABLE III. Summary of the systematic uncertainties.

Source	Relative uncertainty (%)
Tracking efficiency	0.39
Energy requirement	0.09
Momentum requirement	0.43
Polar angle requirement	0.38
MC statistics	0.25
Beam energy	0.42
Trigger efficiency	0.10
Generator	0.50
Total	0.97

VI. CROSS CHECK

To verify the result, a cross check with di-gamma events is performed. The event selection criteria are the same as those used in estimating the systematic uncertainty caused by the tracking efficiency, except for the requirement on $\Delta\phi$. In order to reduce the Bhabha background, the $\Delta\phi$ is required to be in the range of $[-0.8^\circ, 0.8^\circ]$, since photons are not deflected

in the magnetic field.

The luminosity results of this cross check (L_{ck}) are shown in Table I, together with the relative differences to the nominal ones. Both results are well consistent for all individual measurements, indicating the robustness of the result.

VII. SUMMARY

The integrated luminosity of the data samples taken at BE-SIII for studying the charmoniumlike states and higher excited charmonium states is measured to a precision of 1% with Bhabha events. The total uncertainty is dominated by the systematic uncertainty. A cross check with di-gamma events is performed and the results are consistent with each other. The result presented here is essential for future measurements of cross sections with these data, and it has already been used in the discovery of charged charmoniumlike states [10–13].

ACKNOWLEDGMENTS

The BESIII collaboration would like to thank the staff of BEPCII and the IHEP computing center for their strong support. This work is supported in part by National Key Basic Research Program of China under Contract No. 2015CB856700; National Natural Science Foundation of China (NSFC) under Contracts Nos. 11125525, 11235011, 11322544, 11335008, 11425524; the Chinese Academy of Sciences (CAS) Large-Scale Scientific Facility Program; Joint Large-Scale Scientific Facility Funds of the NSFC and CAS under Contracts Nos. 11179007, U1232201, U1332201; CAS under Contracts Nos. KJCX2-YW-N29, KJCX2-YW-N45; 100 Talents Program of CAS; INPAC and Shanghai Key Laboratory for Particle Physics and Cosmology; German Research Foundation DFG under Contract No. Collaborative Research Center CRC-1044; Istituto Nazionale di Fisica Nucleare, Italy; Ministry of Development of Turkey under Contract No. DPT2006K-120470; Russian Foundation for Basic Research under Contract No. 14-07-91152; U.S. Department of Energy under Contracts Nos. DE-FG02-04ER41291, DE-FG02-05ER41374, DE-FG02-94ER40823, DESC0010118; U.S. National Science Foundation; University of Groningen (RuG) and the Helmholtzzentrum fuer Schwerionenforschung GmbH (GSI), Darmstadt; WCU Program of National Research Foundation of Korea under Contract No. R32-2008-000-10155-0.

[1] N. Brambilla, S. Eidelman, B. K. Heltsley, R. Vogt, G. T. Bodwin, E. Eichten, A. D. Frawley and A. B. Meyer *et al.*, *Eur. Phys. J. C* **71** 1534 (2011).
 [2] M. Ablikim *et al.* [BESIII Collaboration], *Chin. Phys. C* **37**, 032007 (2013).

[3] M. Ablikim *et al.* [BESIII Collaboration], *Nucl. Instrum. Meth. A* **614**, 345 (2010).
 [4] S. Agostinelli *et al.* [GEANT4 Collaboration], *Nucl. Instrum. Meth. A* **506**, 250 (2003).
 [5] J. Allison, K. Amako, J. Apostolakis, H. Araujo, P. A. Dubois, M. Asai, G. Barrand and R. Capra *et al.*, *IEEE Trans. Nucl. Sci.*

- 53**, 270 (2006).
- [6] G. Balossini, C. M. Carloni Calame, G. Montagna, O. Nicosini and F. Piccinini, Nucl. Phys. B **758**, 227 (2006).
 - [7] R. G. Ping, Chin. Phys. C **32**, 599 (2008).
 - [8] M. Ablikim *et al.* [BESIII Collaboration], *Measurement of the center-of-mass energy of the data taken by BESIII at center of mass energies between 3.81 GeV and 4.60 GeV*, Paper in preparation.
 - [9] N. Berger, K. Zhu, Z. -A. Liu, D. -P. Jin, H. Xu, W. -X. Gong, K. Wang and G. -F. Cao, Chin. Phys. C **34**, 1779 (2010).
 - [10] M. Ablikim *et al.* [BESIII Collaboration], Phys. Rev. Lett. **110**, 252001 (2013).
 - [11] M. Ablikim *et al.* [BESIII Collaboration], Phys. Rev. Lett. **111**, 242001 (2013).
 - [12] M. Ablikim *et al.* [BESIII Collaboration], Phys. Rev. Lett. **112**, 022001 (2014).
 - [13] M. Ablikim *et al.* [BESIII Collaboration], Phys. Rev. Lett. **112**, 132001 (2014).